CHEMICAL ACTIVITY AND MORPHOLOGY OF NANOSTRUCTURED PLASMA-SPRAYED TITANIUM INDUCED BY NITROGEN AND ARGON IONS

Irina Perinskaya[1], *Vladimir* Perinsky[1], *and Svetlana* Kalganova[1]

[1]Yuri Gagarin State Technical University of Saratov, Saratov, Russia

Abstract. The paper focuses on the chemical characteristics of ion-beam passivation effects (of the first-third order) of titanium depending on the dose of implanted ions. The key objective is electron microscopy and SPM-based analysis of nanostructured VT1-00 titanium surfaces produced by entering nitrogen and argon ions of high energy. This type of surfaces can find application in fabrication of devices for the power engineering industry. The obtained experimental data provide evidence of a carbon nanocoating over the surface of titanium implanted with accelerated nitrogen ions, which is similar to that acquired upon titanium implantation with argon ions. A hypothesis is formulated about the existence of a mechanism for changing the chemical activity of titanium as a result of ion-beam nanostructuring – ion-stimulated synthesis of.

1 Introduction

In recent years, ion implantation, i.e. the process where ions are accelerated into solid bodies, has acquired prime importance not only in designing microelectronic devices for modern solid-state electronics, but also in creating a universal methodology for experimental solid-state physics and materials science, which can be applied in fabrication and research of nanomaterials. Studies of the effects of ion implantation into metals are conducted across many lines, starting from simulation of neutron, proton, and helium defects in the walls of nuclear reactors to the challenges concerned with improving corrosion resistance of copper layers in microwave ICs [1-4]. The development of ion-beam technology is based on experimental findings relating interaction between the fast charged particles and metals, accompanied by the issues relating the passage, restriction, and scattering of ions, i.e. the primary "fast" processes and changes in their morphology, surface structure, and physical-chemical properties. This research is devoted to the study of the VT1-00 nanostructured titanium, induced by the nitrogen and argon ions, which is required in manufacturing power engineering devices.

2 Experimental methods

For the test models we used polished and chemically degreased titanium structures based on the VT1-00 substrate sized 10×10×2 mm, with a titanium layer sprayed by means of the ion-plasma treatment methodology with the dispersion of 3 -5 μm, sputtering distance of 70-80 mm, and thickness of 5 -10 μm. These test models can be applied as workpieces for the power engineering products. Part of the test models underwent ion-beam treatment by nitrogen ions (N^+), a second part was treated by argon ions (Ar^+), with the ion dose at the accelerating voltage amplitude about 75 keV. The technique employs the dynamic process vacuum of ~ $4 \cdot 10^{-3}$ MPa maintained under a controlled carbon gas release (CO_2) in the inlet chamber (Fig. 1) [5]. This experiment was conducted using "Vesuvius-5", an industrial implantation doping unit of Russian manufacture.

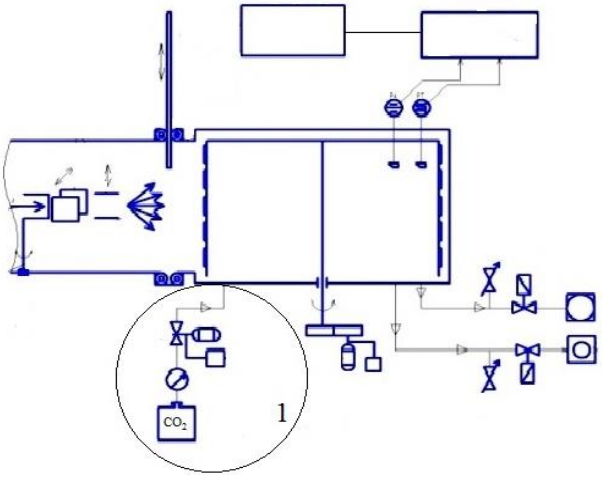

Fig. 1. Diagram of the improved receiving chamber of the "Vesuvius-5" ion doping installation: (1) a point for a controlled inlet of carbon-containing gas (CO_2).

The ion beam with the current density of ~10 μA/cm^2 was used to scan the horizontal and vertical lines of the samples at the frequency of 427 Hz, whereas the heating

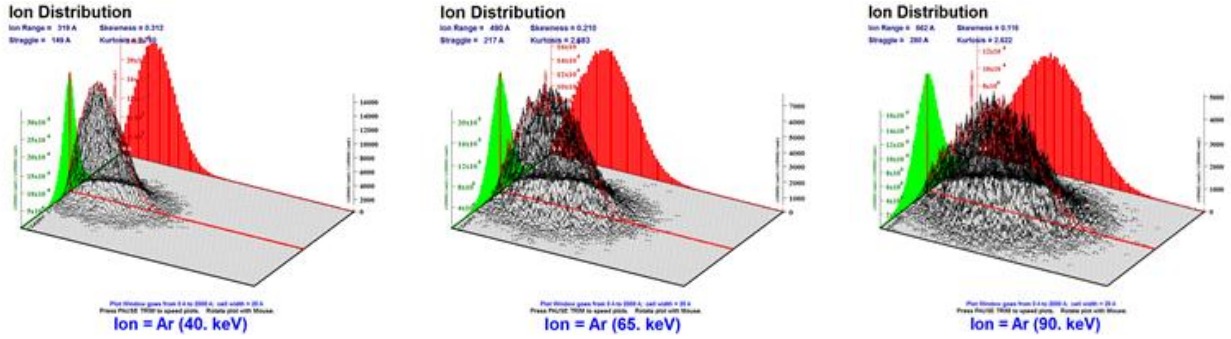

a b c

Fig. 2. 3D distribution profiles of an argon ion beam in the titanium layer with the dose of 10^5 ion/cm^2, and 2D projections of plotted data at the changes in accelerating voltage: (a) U_{acc} =40 keV, and (b) U_{acc} =65 keV; (c)-U_{acc} =90 keV.

temperature for the samples in the course of ion-beam processing did not exceed 80°C.

A research was made into dependence of the relative chemical etching rate (V) of titanium on the dose of argon and nitrogen ions. The relative chemical etching rate (relation between the chemical etching rate of non-irradiated V_0 and ion-irradiated V_{irr} parts of the samples) can be defined by the ratio: $V=V_{irr} / V_0 = t_0 / t_{irr}$, where t_0, t_{irr},V_0, V_{irr} are the time and rate of the chemical etching of corresponding parts of the samples.

The ion-beam chemical passivation effect corresponds to the relative chemical etching rate V<1, and activation effect rate V>1.

Chemical etching of the test models was performed at room temperature in the liquid etchant standard for titanium.

On completing the ion-beam treatment, morphology of the test models was studied using the following means: the TESCAN MIRA II LMU scanning electron microscope (SEM) under accelerating voltage of 30 keV, the JSM-6701F scanning electron microscope equipped with a cold field emission source (PE-SEM), electronic energy loss in front of the sample, and the negative retarding potential applied to the sample up to 2 keV utilized to examine the nanostructures, and the SMM-2000 scanning probe microscope.

The provided computer simulation results help to visualize the dynamic ion-beam treatment procedure, and set into correspondence the ion beam parameters with the processing characteristics of the modified target.

While investigating the dependence of a relative chemical etching rate of titanium on the dose of argon and nitrogen ions, the period of total etching of un-irradiated (t0) and ion-irradiated (tirr) areas of the deposited titanium layer was under control (Fig. 3).

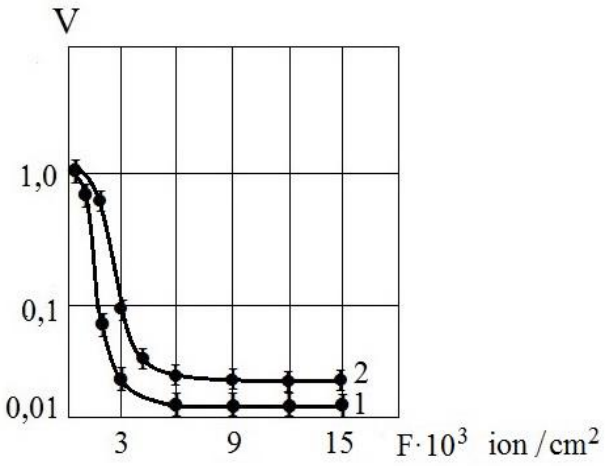

Fig. 3. Dependence of the relative chemical etching rate of titanium on the ion dose: (1) argon, and (2) nitrogen (Uacc=75keV).

The titanium surface morphology of the test models was investigated in the course of nitrogen and argon ion dosing procedures (Fig. 4,5).

The conducted experimental research indicates the existence evidence of a mechanism that enables changes in the structure and physical-chemical properties of implanted materials. The key mechanisms manifesting significant transformations in the nanostructure of materials are as follows:

- changes in the interaction characteristic between the metal surfaces and external environment [7];
- changes in the physical and chemical properties of the existing surfaces, and formation of new internal surfaces within the implanted metals [8];
- changes in the phase and chemical composition of metals [8];
- radiation-enhanced nanostructural transformations in the metal volumes [9].

The changes found in the morphology of titanium surfaces, undergoing in the process of ion-beam treatment within the carbon-containing gas (CO_2) medium, depend on the dose of nitrogen and argon ions. At the ion dose lower than the "critical" ~3000 μCl/cm^2,

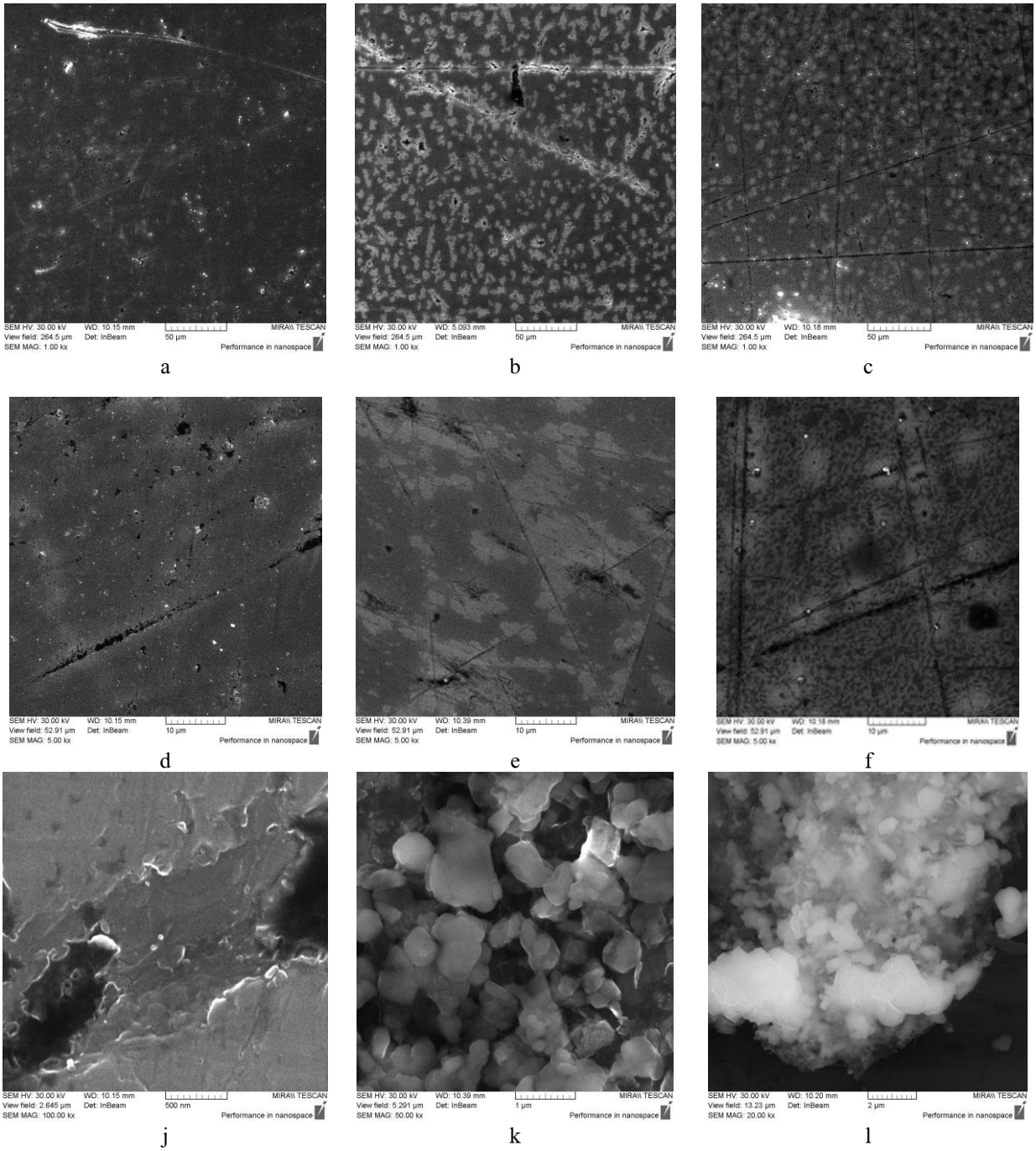

Fig. 4. The images of titanium surface in the scanning electron microscope: (a, d, g, j) before the ion-beam treatment procedure, (b, e, h, k) after ion-beam treatment by nitrogen ions of F=1000 μCL/cm^2, and (c, f, i, l) after ion-beam treatment by the nitrogen ions of F=10000 μCL/cm^2.

a microcrystalline film with the most noticeable triangular {111} planes is formed (Fig. 5 (a),(b). This film has a polycrystalline nature due to crystal twinning and numerous crystalline fractures. The nanorelief of the film synthesized on the titanium surface by argon ion implantation can be examined using the JSM-6701F PE-REM with the resolution of at least 15 nm (Fig. 5, d).

Morphological characteristics of the surface of titanium samples were investigated using the scanning probe microscopy.

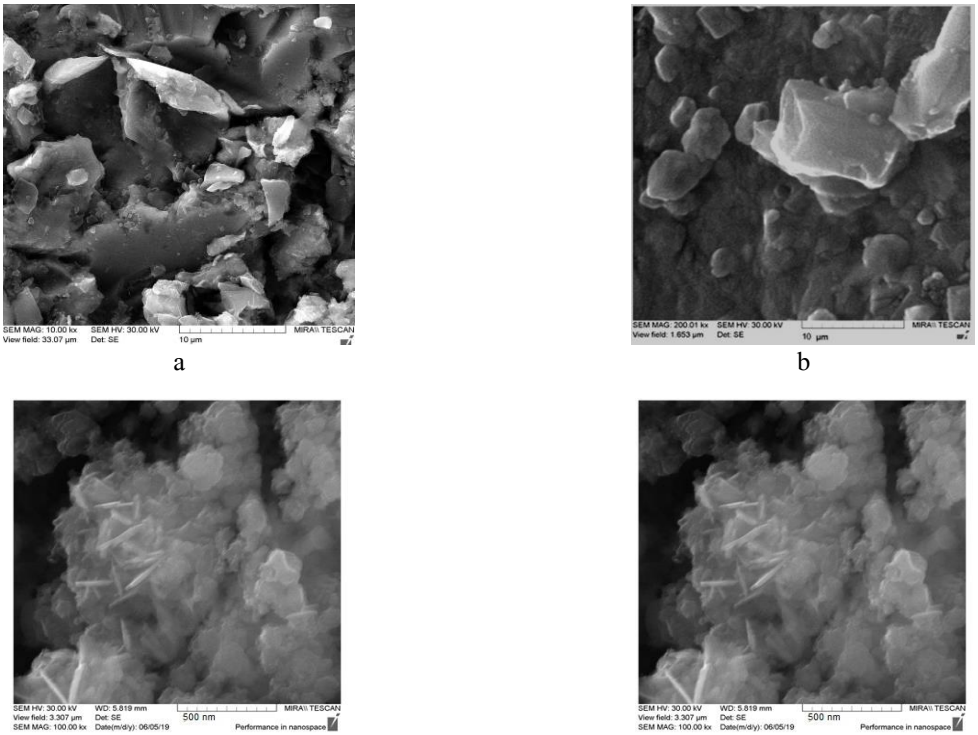

Fig. 5. A scanning electron microscope image with a cold-field emission (U_{acc} =75 kV): (a) a microcrystalline film on the titanium surface after the ion-beam treatment $Ar^+$with F=2000 μCL/cm^2, (b) a microcrystalline film on the titanium surface after the ion-beam treatment Ar^+ with F=2500 μCL/cm^2, (c) the film demonstrating a "cauliflower" morphology on the titanium surface after the ion-beam treatment Ar^+ with P=3000 μCr/cm^2, and (d) morphology of a nanoscale film synthesized on the titanium surface after the ion-beam treatment Ar^+ with P=5000 μCr/cm^2 (the dose conversion factor: 1μCL/cm^2 =6,23-10^{12} ion/cm^2).

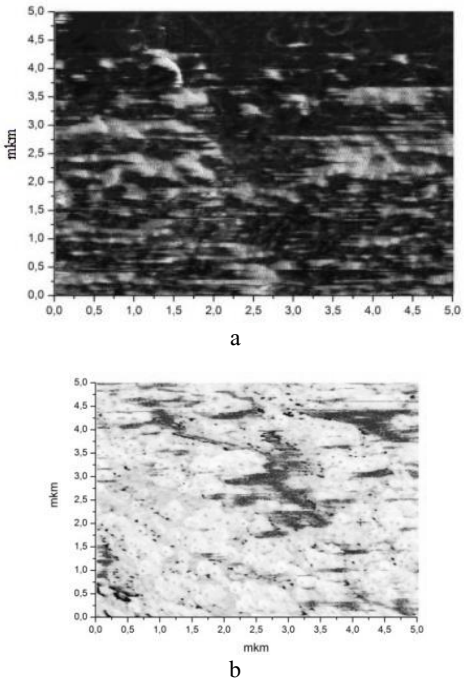

Fig. 6. SPM-photographs of the surface of titanium samples: (a) initial state, and (b) after the ion-beam surface treatment with the nitrogen ions N+ (F=5000 μCl/cm^2).

Figure 7 shows a 3D image of the titanium surface before and after ion-beam nanostructuring procedure using nitrogen ions.

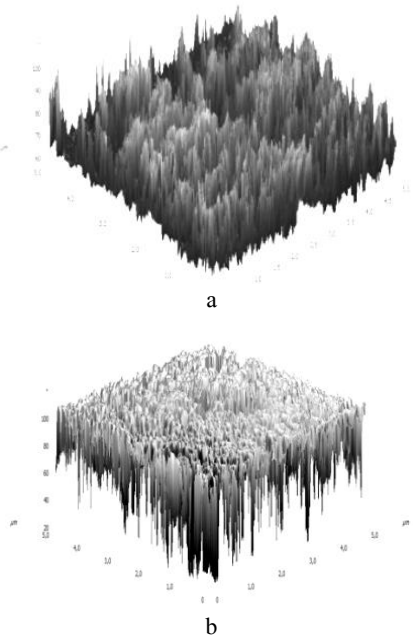

Fig. 7. 3D image of the titanium surface: (a) initial sample, and (b) a sample implanted with nitrogen ions F=10000 μCl/cm^2).

The study of titanium morphology based on the scanning probe microscopy showed that radiation with nitrogen ions in the dynamic technological vacuum ~ $4 \cdot 10^{-4}$ Pa, with controlled use of CO_2, provides modifications in the surface layer (Fig. 6). Figure 7 shows an SPM image of the titanium surface obtained by means of the image processing module Nova. The coating formed as a result of ion irradiation consists of vertical structures.

Application of the secondary ion mass spectrometry technique helped to establish that carbon, oxygen, and nitrogen are the main contaminants contained in the primary metal layers. Chlorine, sulfur, and calcium peaks are also recorded over the surface of the samples; they vanish after the surface is treated with accelerated ion beams.

After ion irradiation at energies and dose levels around ~1500-10000 μCL/cm^2, the amount of carbon in all the test models of titanium coatings, as compared to significant amounts, increases by 20-30%, whereas oxygen and nitrogen impurities are redistributed. Analysis of the Auger peak shape shows that carbon, inside implanted layers, is found in the bound state, presumably, in the shape of metal carbides. An increase in the amount of carbon on the surface of implanted layers can be attributed to its segregation from the metal body, as well as condensation of carbon-containing fragments from the vacuum chamber space containing carbon gas (CO_2).

Thus, as a result of plasma-sprayed treatment of titanium, either by nitrogen or argon ions, a nanoscale carbon-containing coating is formed over its surface.

3 Conclusions

The conducted experiments resulted in the research into plasma-sprayed commercially pure VT1-00 titanium samples irradiated with argon and nitrogen ions. Additionally, physical and chemical characteristics of the effect (first-third order) of ion-beam passivation, depending on the dose of argon or nitrogen ions, were established. Regarding its quality, the passivation effect V<1, at either nitrogen ion or argon ion implantation, is similar. It is characterized by an exponentially rapid slowdown in the chemical etching rate near the threshold dose, and an increase in the amount of carbon in the material under study.

Investigation of electron microscopic (SEM, PE-REM), SEM images of the titanium surface nanostructured by accelerated ions, provide evidence for the presence of superthin carbon nanocoatings over titanium surfaces implanted with nitrogen ions. Similar surfaces are found in the titanium implanted with argon ions. The presented research results confirm our hypothesis relating a second mechanism that changes the chemical activity of titanium as a result of ion-beam nanostructuring, i.e. ion-stimulated synthesis of nanoscale carbon-containing films.

Figures and tables, as originals of good quality and well contrasted, are to be in their final form, ready for reproduction, pasted in the appropriate place in the text. Try to ensure that the size of the text in your figures is approximately the same size as the main text (10 point). Try to ensure that lines are no thinner than 0.25 point.

References

1. A.I. Ryabchikov, E.B. Kashkarov, A.E. Shevelev, A. Obrosov, D.O. Sivin, Surface and Coatings Technology, **372**, 1-8 (2019)
2. R.A. Nazipov, R.I. Batalov, R.M. Bayazitov, H.A. Novikov, Journal of Physics: Conference Series, **1**, 1588 (2019)
3. I.V. Perinskaya, V.V. Perinsky, Inorganic Materials: Applied Research, **11**, 721-726 (2020)
4. C.-Y. Lee, P.-C. Lin, C.-H Yang, C.-E. Ho, Surface and Coatings Technology, **386**, 125471 (2020)
5. L. Simonot, F. Chabanais, F. Pailloux, S. Rousselet, S. Camelio, D. Babonneau, Applied Surface Science, **544**, 148672 (2021)
6. C. Zhang, J. Li, A. Belianinov, Z. Ma, C.K. Renshaw, R.M. Gelfand, Nanotechnology, **46**, 465302 (2020)
7. I.V. Perinskaya, Perspektivnyye materialy, **5**, 45-49 (2009)
8. I.V. Perinskaya, I.V. Rodionov, L.E. Kuts, Patent RF na poleznuyu model **176553** (23 January 2018)
9. I.E. Ziegler, Nucl. Instr. Meth. Phys. Res. B., **268**, 1818-1823 (2010)
10. S. Ghyngazov, V. Ovchinnikov, V. Kostenko, N. Gushchina, F. Makhinko, Surface and Coatings Technology, **388**, 125598 (2020)
11. K. Barienti, C. Kahra, S. Herbst, F. Nürnberger, H.J. Maier, Metallography, Microstructure, and Analysis, **9**, 54-60 (2020)
12. S. Ghyngazov, V.Kostenko, S. Shevelev, E. Lysenko, Nuclear Instruments and Methods in Physics Research, Section B, **464**, 89-94 (2020)
13. V. Nelyub, V. Tarasov, Materials and Manufacturing Processes, **172-178**, 35 (2020)
14. Y.F. Ivanov, V.E. Gromov, D.V. Zaguliaev, S.V. Konovalov, Y.A. Rubannikova, A.P. Semin, Progress in Physics of Metals, **345-362**, 21 (2020)
15. T.I. Dorofeeva, T.A. Gubaydulina, O.V. Sergeev, A.P. Sungatulin, V.P. Sergeev, IP Conference Proceedings, **2167**, 020073(2019)
16. I.V. Perinskaya, I.V. Rodionov, L.E. Kuts, Inorganic Materials: Applied Research, **10**, 347-353 (2019)
17. Z. Li, F. Chen, Applied Physics Reviews, **4**, 011103 (2017)
18. B.A. Kalin, N.V. Volkov, R.A. Valikov, A.S. Yashin, V.P. Krivobokov, S.N. Yanin, O.K Asainov, Y.N. Yurev, IOP Conference Series: Materials Science and Engineering, **130**, 012051 (2016)